Multiple Solutions in the Theory of DC Glow Discharges

Pedro G. C. Almeida* and Mikhail S. Benilov
Departamento de Física, Universidade da Madeira
*Corresponding author: Departamento de Física, Universidade da Madeira, Largo do Município 9000 Funchal, Portugal, pedroa@uma.pt

Abstract: It has been suggested long ago that a theoretical model of a near-cathode region in a DC glow discharge admits multiple steady-state solutions describing different modes of currrent transfer. Even the most simple self-consistent models should admit such multiple solutions. In the present work, these solutions have been calculated for the first time.

Keywords: Glow discharge, plasma-cathode interaction, Self-organization

1. Introduction

It is well known that current transfer to cathodes of DC glow discharges can occur in the abnormal mode or in the mode with a normal spot, e.g. [1]. This has led to a hypothesis [2] that a self-consistent theoretical model of a near-cathode region in a DC glow discharge admits multiple steady-state solutions describing different modes of current transfer. Recent observations of patterns of more than one spot in DC glow microdischarges [3-7] can be interpreted as another argument in favour of this hypothesis [8]. A bifurcation analysis [9] has shown that multiple steady-state solutions must exist even in the framework of the most basic self-consistent model of a glow discharge, which is a discharge between parallel electrodes with a single ion species and transport of the ions and the electrons dominated by drift, without account of complex effects such as a nonlocal electron energy distribution or the presence of multiple ion and neutral species with a complex chemistry.

In the present work, multiple steady-state solutions are found for the first time.

2. The Model

The simplest self-consistent mathematical model of a DC glow discharge comprises equations of conservation of a single ion species and electrons, transport equations for the ions and the electrons written in the so-called drift-diffusion approximation (i.e., neglecting inertia of the charged particles; e.g., [10]), and the Poisson equation:

$$\nabla \cdot \mathbf{J}_i = n_e \alpha \mu_e E - \beta n_e n_i, \qquad \mathbf{J}_i = -D_i \nabla n_i - n_i \mu_i \nabla \varphi, \tag{1}$$

$$\nabla \cdot \mathbf{J}_e = n_e \alpha \mu_e E - \beta n_e n_i, \qquad \mathbf{J}_e = -D_e \nabla n_e + n_e \mu_e \nabla \varphi, \tag{2}$$

$$\varepsilon_0 \nabla^2 \varphi = -e\left(n_i - n_e\right). \tag{3}$$

Here n_i, n_e, $\mathbf{J}_i$, $\mathbf{J}_e$, D_i, D_e, μ_i, and μ_e are number densities, densities of transport fluxes, diffusion coefficients, and mobilities of ions and electrons, respectively; α is Townsend's ionization coefficient; β is coefficient of dissociative recombination; φ is electrostatic potential, $E = |\nabla \varphi|$ is electric field strength; ε_0 is permittivity of free space; and e is elementary charge. Processes considered for volume ionization and recombination are electron impact ionization and dissociative recombination.

Let us assume that the discharge vessel represents a right circular cylinder of a radius R and of a height h, and introduce cylindrical coordinates (r, ϕ, z) with the origin at the center of the cathode and the z-axis coinciding with the axis of the vessel. Boundary conditions at the cathode, anode, and walls of the discharge vessel are written, respectively, as

$$z = 0: \quad \frac{\partial n_i}{\partial z} = 0, \quad \left(\mathbf{J}_e\right)_z = -\gamma\left(\mathbf{J}_i\right)_z, \ \varphi = 0; \tag{4}$$

$$z = h: \quad n_i = 0, \ \frac{\partial n_e}{\partial z} = 0, \ \varphi = U; \tag{5}$$

$$r = R: \quad \frac{\partial n_i}{\partial r} = \frac{\partial n_e}{\partial r} = 0, \ \left(\mathbf{J}_e + \mathbf{J}_i\right)_r = 0. \tag{6}$$

Here γ is the effective secondary emission coefficient and U is the discharge voltage. Note that the condition of vanishing ion number density at the anode surface, $n_i = 0$, represents an adequate boundary condition on an absorbing non-emitting and non-reflecting surface in the framework of the drift-diffusion approximation (e.g., Appendix B of [11] and references therein). In principle, it would be natural to apply this condition also at the cathode. However, there is a computational difficulty: a solution obtained in such way contains the so-called ion diffusion layer [12, 13], which is a very thin region positioned immediately in front of the cathode surface "at the bottom" of the space-charge sheath where n_i sharply drops, and a numerical resolution of this layer is costly. On the other hand, thickness of this layer as described by the drift-diffusion approximation is usually below the ion mean free path; an indication that the drift-diffusion description is not valid and one should resort to a kinetic description [14]. Besides, this layer, being very thin, is unimportant for an accurate description of the discharge on the whole. Therefore, the boundary condition for n_i at the cathode is usually written in the form of zero normal derivative (e.g., [15]), which eliminates the ion diffusion layer. The latter boundary condition is used also in this work, and a similar boundary condition is applied to n_e at the anode. These boundary conditions are applied also at the walls, which amounts to neglecting diffusion losses to the walls; a case in which the pattern of multiple solutions is more straightforward. (A change of this pattern which will occur if the diffusion losses are taken into account will be discussed below.) The last boundary condition in (6) means that the walls are electrically insulating. Note that the boundary conditions in the form (4)-(6) have been used in [16] in a numerical investigation of a glow discharge in molecular nitrogen burning in the mode of normal current density.

The input parameters for the model can be both the discharge voltage U or the discharge current. Both possibilities have been used in the calculations, depending on the differential resistance of the discharge at the state being modelled.

The problem (1)-(6) is well known and represents the most basic self-consistent model of a DC glow discharge. This problem admits a 1D solution of the form $f = f(z)$ (here f is any of the functions n_i, n_e, and φ) which is in essence the well-known solution of von Engel and Steenbeck [1]. In certain conditions, the problem admits also 2D (axially symmetric) solutions, $f = (r, z)$, and 3D solutions, $f = f(r, \phi, z)$. In this work, 2D solutions are found.

The model was implemented in COMSOL Multiphysics through a coupling between two convection-diffusion application modes and one electrostatic application mode.

3. Results and discussion

As an example, let us consider results for a discharge in xenon under the pressure of 30Torr in a discharge tube with $R = h = 0.5mm$. The mobility of Xe^{+2} ions in Xe was evaluated by means of the formula $\mu_i = 2.1\times10^{21}\, m^{-1} V^{-1} s^{-1}/n_n$ (here n_n is the density of the neutral gas), which is an approximation of the measurements [17]. The mobility of the electrons was evaluated by the formula $\mu e = 19$ Torr $m^{-2} V^{-1} s^{-1}/p$, where p is the pressure of the plasma; Townsend's ionization coefficient α was evaluated by equation (4.6) of [1]. (Note that this way of evaluation of μ_e and α yields results in good agreement with those given by the zero-dimensional Boltzmann solver BOLSIG [18].) The diffusion coefficients were evaluated by means of Einstein's law, $D_{i,e} = kT_{i,e}\, \mu_{i,e}/e$, where k is Boltzmann's constant and T_i and T_e are temperatures of the heavy particles and electrons, respectively: $T_i = 300\ K$ and $T_e = 1\ eV$. The coefficient of dissociative recombination of molecular ions Xe^{+2} was set equal to $2\times10^{-13}\ m^3 s^{-1}$ [19, 20]. The effective secondary emission coefficient was set equal to 0.03.

Current-voltage characteristics (CVCs) of the 1D solution and two 2D solutions are shown in figures 1 and 2 . Here $\langle j \rangle$ is the average value of the axial component of the electric current density evaluated over the (circular) cross section of the discharge vessel. The full line in both figures represents the CVC corresponding to the 1D solution. This is essentially the well-known solution of von Engel and Steenbeck [1]; it exists at all values of the discharge current and describes states corresponding to: (i) the Townsend discharge at low currents, $\langle j \rangle < 1\ A\ m^{-2}$; (ii) the falling part of the CVC,

which is usually assumed to be unstable; and (iii) the abnormal glow discharge, with a rising CVC.

The CVC of one of the 2D solutions is shown in figure 1. A part of this CVC is shown by the dashed line and a part by the dotted line. The CVC of the other 2D solution is shown in figure 2, also by the dashed and dotted lines. Each of the 2D solutions exists only in a limited range of the discharge currents and its CVC represents a closed curve.

For the 2D solution shown in figure 1, there are two states in which functions n_i, n_e, and φ vary with z but not with r. These states are marked by triangles; one is close to the point of minimum of the CVC of the 1D solution and is designated *a*, the other is close to the Townsend regime and is designated *d*. These states belong not only to the 2D solution being considered, but also to the 1D solution. This phenomenon is well known in mathematical physics and is called bifurcation, or branching of solutions, and states at which it occurs are called bifurcation points. The 2D solution shown in figure 2 also possesses two bifurcation points, which are marked in both figures 1 and 2 and are designated *b* and *c*. In all the cases, the 2D solution exists at currents both below and above the current value that corresponds to the bifurcation point; in other words, the bifurcation is transcritical in accord to the theoretical predictions [9].

In agreement to the bifurcation theory [9], each 2D solution in the vicinity of a bifurcation point represents a superposition of a 1D distribution and a small 2D perturbation with the radial variation governed by the Bessel function of the first kind and zeroth order, $J_0(k\,r)$, where $k = 3.832/R$ and $k = 7.016/R$ for the 2D solutions shown in figures 1 and 2, respectively. [Note that numbers 3.832 and 7.016 represent abscissas of the first 3 minimum and the first maximum of the function $J_0(x)$ inside the interval $0 < x < 1$.] In the following, the 2D solutions shown in figures 1 and 2 will be referred to as, respectively, the first and second 2D modes.

One can see from figure 1 that the bifurcation points of the second mode, *b* and *c*, are shifted in the direction towards each other as compared to the bifurcation points of the first mode, *a* and *d*. Accordingly, the range of currents in which the second 2D mode exists is narrower than the range of existence of the first mode. This is a

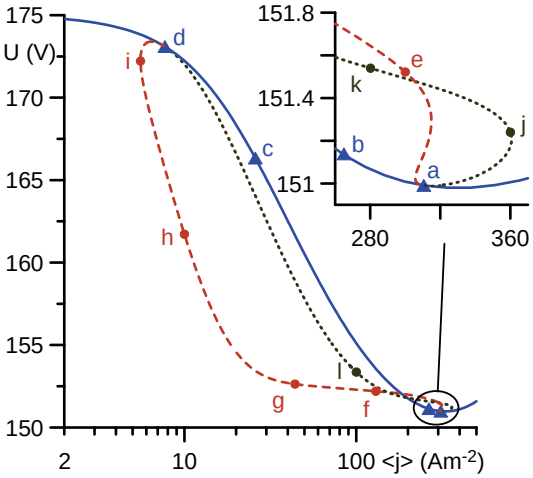

Figure 1. CVCs. Full line: 1D solution. Dashed, dotted lines: the first 2D mode. Triangles: bifurcation points at which the first (a, d) and second (b, c) 2D modes branch off from the 1D solution. Circles: states for which the distributions of current density over the cathode surface are shown in figures 3 or 5.

behaviour typical for bistable nonlinear dissipative systems; see figure 2 [21]. (Note that the two stable regimes of the considered system are represented by the abnormal discharge and the situation where the discharge has not been ignited [8].) Calculations not shown here demonstrate that this shrinking of the existence range is responsible for the fact that no

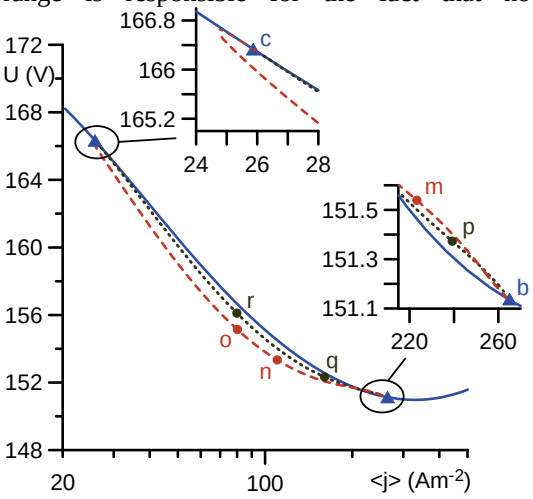

Figure 2. CVCs. Full line: 1D solution. Dashed, dotted lines: the second 2D mode. Triangles: bifurcation points at which the second 2D mode branches off from the 1D solution. Circles: states for which the distributions of the current density over the cathode surface are shown in figure 4.

higher-mode 2D solution exist.

Images of the distribution of (local) current density j over the cathode surface are shown in figures 3 and 4. States to which every image in these figures corresponds are indicated in figures1 and 2. The dashed line in figure 1 corresponds to states with a spot at the center of the cathode surface, while the dotted line corresponds to states with a ring spot at the periphery of the cathode. The dashed line in figure 2 corresponds to states with a spot at the center of the cathode and a ring spot at its periphery, while the dotted line corresponds to states with a ring spot in the interior of the cathode surface. One can conclude that there are two self-organization patterns corresponding to each 2D mode with the switching between the patterns occurring at each bifurcation point. In the following, the sections of the first 2D mode which are represented in figure 1 by the dashed and dotted lines will be referred to as, respectively, the branch with a central spot and the branch with a ring spot at the periphery of the cathode. The sections of the second 2D mode represented in figure 2 by the dashed and dotted lines will be referred to as, respectively, the branch with a central spot and a ring spot, and the branch with an interior ring spot.

Evolution of each pattern along the corresponding branch from one bifurcation point to the other follows the same scenario: on leaving the bifurcation point in the vicinity of the point of minimum of the CVC of the 1D solution, j increases at certain positions of the cathode and decreases at others, thus a spot system is formed. As the distance from the bifurcation point increases, the spots shrink; their brightness first increases and then starts

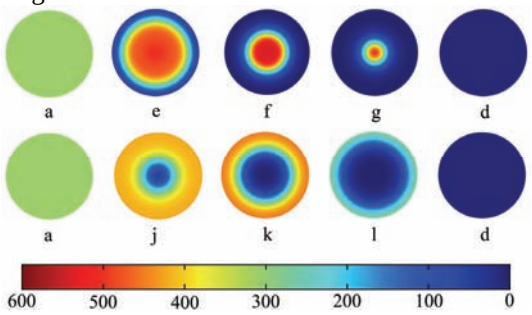

Figure 3. Images representing distributions of the current density over the cathode surface in the first 2D mode. The bar is in A m^{-2}.

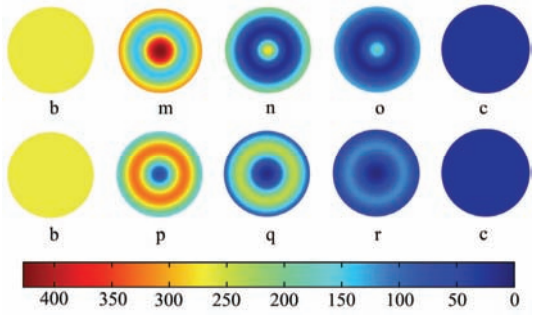

Figure 4. Images representing distributions of the current density over the cathode surface in the second 2D mode. The bar is in A m^{-2}.

decreasing. When the latter occurs, the spots become less pronounced. In the vicinity of the second bifurcation point, the spots completely disappear.

Evolution of the pattern with a central spot, which is illustrated by the first set of five images in figure 3 and also by figure 5, is of particular interest. (States to which every image in figure 5 corresponds are indicated in figure 1.) The spot is formed between states *a* and *e*. The spot shrinks between states *e* and *g*, however the current density inside the spot remains more or less constant, i.e., a decrease of the electric current is accompanied by a decrease of the area of the spot. After state *g*, the current density in the spot starts decreasing. The current density on the periphery of the cathode decreases between *a* and *h* and after state *h* starts increasing. After state *h*, the non-uniformity of the current distribution over the cathode decreases, and the distribution at state *i* is already rather smooth. The spot is completely extinguished between states *i* and *d*.

The above-described constancy of j inside the spot between states *e* and *g* is associated with the plateau of the CVC represented by the dashed line in figure 1. (While the average current density $\langle j \rangle$ decreases from 300 $A\ m^{-2}$ at state *e* to 44 $A\ m^{-2}$ at state *g*, the discharge voltage varies only from 151.5 V to 152.6 V.) Both these features are characteristic for the effect of normal current density; e.g. [1]. Hence, the central-spot branch between states *e* and *g* may be identified with the normal mode.

At the point of minimum of the CVC of the 1D solution, j = 323 $A\ m^{-2}$. Values of the current density inside the normal spot considerably exceed this value and more or less correspond to

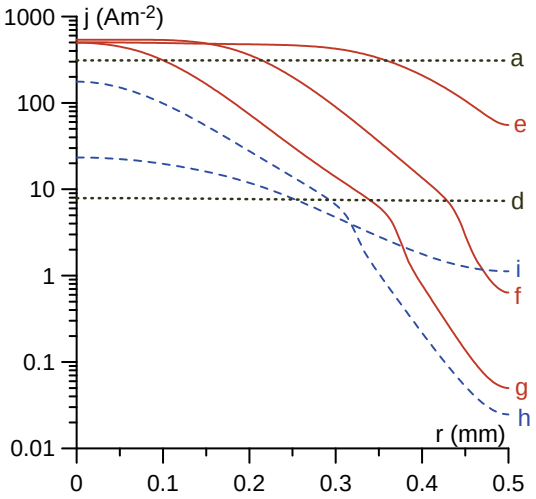

Figure 5. Distributions of the current density over the cathode surface on the central-spot branch of the first 2D mode.

values of the current density that occur on the abnormal mode at the same discharge voltage. For example, the value of discharge voltage U at state e is 151.5 V . At this U, the current density in the abnormal mode equals 490 $A\ m^{-2}$, which is not very different from the maximum value of j at state e, equal to 503 $A\ m^{-2}$. Similarly, U = 152.2 V at state f ; the current density at this U in the abnormal mode equals 593 $A\ m^{-2}$ and is not dramatically different from the maximum value of j at state f, which is 539 $A\ m^{-2}$. Hence, one one can view the effect of normal current density as a manifestation of coexistence of a hot phase, representing the abnormal mode, with a cold phase, representing a situation in which no discharge is present at the cathode surface point being considered. Note that the concept of coexistence of phases is a useful tool well-known in theoretical physics; in particular, this concept gives a hint as to why the discharge voltage is virtually constant in the normal mode: the coexistence of phases is usually possible at only one value of the control parameter, in our case, U.

The effect of normal current density occurs also at the branch with a ring spot at the periphery, although in a narrower range of the discharge currents: when the average current density $\langle j \rangle$ on this branch varies from 346 $A\ m^{-2}$ to 275 $A\ m^{-2}$, the discharge voltage varies from 151.4 V to 151.6 V and the maximum current density from 445 $A\ m^{-2}$ to 452 $A\ m^{-2}$. No effect of normal current density is present on branches of the second 2D mode. The patterns with a ring spot or with a central spot and a ring spot may be viewed as axially symmetric analogues of patterns observed recently in DC glow microdischarges [3–7]. Thus, the present modelling supports the hypothesis [8] that patterns with multiple spots may be described in the framework of basic mechanisms of glow discharge, so there is no need to introduce special mechanisms to this end.

As values of the diffusion coefficients D_i and D_e are reduced, the bifurcation point at which the first 2D mode branches off (point a in figure 1) is shifted in the direction of higher j. When diffusion is neglected completely, this point has been shifted to j = 363 $A\ m^{-2}$. The latter value conforms to the one at which the first axially symmetric bifurcation occurs in the framework of the bifurcation theory [9], which is j = 367 $A\ m^{-2}$. Furthermore, this bifurcation point belongs to the rising section of the CVC of the 1D solution, since the minimum of the CVC of the 1D solution without diffusion occurs at j = 318 $A\ m^{-2}$. Thus, the present modelling has confirmed the possibility of a bifurcation on a discharge mode with a positive differential resistance; a result very interesting theoretically.

When diffusion losses to the walls are taken into account, the von Engel and Steenbeck solution is no more 1D but becomes 2D (axially symmetric), i.e., distributions of n_i, n_e, and φ become functions of both z and r. Judging by analogy with cathodes of arc discharges [22], one can expect that the 2D solutions describing different spot patterns will continue to exist, although they will be disconnected from the von Engel and Steenbeck solution.

4. Conclusion

Multiple steady-state solutions have been found in the framework of the simplest self-consistent glow discharge model. One is a 1D solution, which is essentially the well-known solution of von Engel and Steenbeck, and the others are axially symmetric solutions describing patterns with: a spot at the center of the cathode; a ring spot at the periphery of the cathode; a spot at the center and a ring-spot at the periphery of the cathode; an interior ring spot.

The mode with a spot at the center of the cathode exhibits all the features of the effect of normal current density and may be viewed as a

manifestation of coexistence of a hot phase, representing the abnormal mode, with a cold phase, representing a situation in which no discharge is present at the point of the cathode surface being considered. The other axially symmetric modes represent axially symmetric analogues of patterns observed recently in DC glow microdischarges.

Future work includes finding 3D solutions, studying stability of 2D and 3D solutions, and eventually taking into account more complex effects such as the presence of multiple ion and/or neutral species and variations of the electron and heavy particle temperatures (similarly to how it is done, e.g., in [16, 23, 24]) with the aim of explaining why patterns with multiple spots have been observed in xenon microdischarges and not in other discharges.

8. References

1. Raizer Y P, *Gas Discharge Physics*, Springer Berlin, (1991)
2. Benilov M S, On the Branching of Solutions in the Theory of the Cathode Sheath of a Glow Discharge, *Sov. Phys. - Tech. Phy*, **33**, 1267-1270 (1988)
3. Schoenbach K H, Moselhy M and Shi W, Self-organization in cathode boundary layer microdischarges, *Plasma Sources Sci. Technol*, **13,** 177-185 (2004)
4. Moselhy M and Schoenbach K H, Excimer emission from cathode boundary layer discharges, *J. Appl. Phys*, **95**, 1642-1649 (2004)
5. Takano N and Schoenbach K H, Self-organization in cathode boundary layer discharges in xenon, *Plasma Sources Sci. Technol*, **15**, S109-S117 (2006)
6. Lee B J, Rahaman H, Frank K, Mares L and Biborosch D L, Properties of the MHCD in Xenon, *Proc. 28th ICPIG* (Prague, July 2007) ed Schmidt J, Šimek M, Pekárek S and Prukner V, Institute of Plasma Physics AS CR, ISBN 978-80-87026-01-4, Prague, 900-902 (2007)
7. Zhu W, Takano N, Schoenbach K H, Guru D, McLaren J, Heberlein J, May R and Cooper J R, Direct current planar excimer source, *J. Phys. D: Appl. Phys*, **40**, 3896-3906 (2007)
8. Benilov M S, Comment on 'Self-organization in cathode boundary layer discharges in xenon' and 'Self-organization in cathode boundary layer microdischarges', *Plasma Sources Sci. Technol*, **16**, 422-425 (2007)
9. Benilov M S, Bifurcations of current transfer through a collisional sheath with ionization and self-organization on glow cathodes, *Phys. Rev. E*, **77** 036408, 1-18 (2008)
10. Kim H C, Iza F, Yang S S, Radmilovic-Radjenovic M and Lee J K, Particle and fluid simulations of low-temperature plasma discharges: benchmarks and kinetic effects, *J. Phys. D: Appl. Phys*, **38**, R283—R301 (2005)
11. Benilov M S and Naidis G V, Ionization Layer at the Edge of a Fully Ionized Plasma, *Phys. Rev. E*, **57**, 2230–2241 (1998)
12. Su C H and Lam S H, Continuum Theory of Spherical Electrostatic Probes, *Phys. Fluids*, **6**, 1479–1491 (1963)
13. Bush W B and Fendell F E, Continuum theory of spherical electrostatic probes. ("frozen" chemistry), *J. Plasma Phys*, **4**, 317 (1970)
14. Benilov M S, Lyashko A V and Kovbasyuk V I, Theory of ion Knudsen near- electrode layer, *Proc. X Int. Conf. on MHD Electrical Power Generation (Tiruchirapalli, India, Dec. 1989)*, **2**, X105–X109 (1989)
15. Boeuf J P and Pitchford L C, Two-dimensional model of a capacitively coupled rf discharge and comparisons with experiments in the Gaseous Electronics Conference reference reactor, *Physical Review E*, **51**, 1376–1390 (1995)
16. Surzhikov S T, Numerical Simulation of Two-Dimensional Structure of Glow Discharge in View of the Heating of Neutral Gas, *High Temp*, **43**, 825–842 (2005)
17. Biondi M A and Chanin L M, Mobilities of Atomic and Molecular Ions in the Noble Gases, Phys. Rev, 94, 910–916 (1954)
18. Pitchford L C, Boeuf J P and Morgan W L Boltzmann simulation software and database http://www.cpat.upstlse.fr/operations/operation 03/POSTERS/BOLSIG/ (1998)
19. Meunier J, Belenguer P and Boeuf J P, Numerical model of an AC plasma display panel cell in neon-xenon mixtures, J. Appl. Phys, 78, 731–745 (1995)

20. Fridman A and Kennedy L A, *Plasma Physics and Engineering*, Taylor and Francis, New York (2004)
21. Benilov M S, Nonlinear Surface Heating of a Plane Sample And Modes of Current Transfer to Hot Arc Cathodes, *Phys. Rev. E*, **58**, 6480–6494 (1998)
22. Benilov M S and Cunha M D, Heating of Refractory Cathodes by High-Pressure Arc Plasmas: II, *J. Phys. D: Appl. Phys*, **36**, 603–614 (2003)
23. Arslanbekov R R and Kolobov V I, Two-dimensional simulations of the transition from Townsend to glow discharge and subnormal oscillations, *J. Phys. D: Appl. Phys*, **36**, 2986–2994 (2003)
24. Boeuf J P, Pitchford L C and Schoenbach K H, Predicted properties of microhollow cathode discharges in xenon, *Appl. Phys.* Lett, **86**, 071501 (2005)

9. Acknowledgements

The work was performed within activities of the projects PPCDT/FIS/60526/2004 and Centro de Ciências Matemáticas of FCT, POCTI-219 and FEDER. Pedro G. C. Almeida was supported by FCT through grant SFRH/BD/30598/2006.